OL Organic Letters

pubs.acs.org/OrgLett Letter

Photophysical Tuning of Shortwave Infrared Flavylium Heptamethine Dyes via Substituent Placement

Monica Pengshung, Jingbai Li, Fatemah Mukadum, Steven A. Lopez,* and Ellen M. Sletten*

Cite This: *Org. Lett.* 2020, 22, 6150−6154 Read Online

ACCESS | Metrics & More | Article Recommendations | Supporting Information

ABSTRACT: Optical imaging in the shortwave infrared region (SWIR, 1000−2000 nm) provides high-resolution images in complex systems. Here we explore substituent placement on dimethylamino flavylium polymethine dyes, a class of SWIR fluorophores. We find that the position of the substituent significantly affects the λ_{max} and fluorescence quantum yield. Quantum-mechanical calculations suggest that steric clashes control the extent of π-conjugation. These insights provide design principles for the development of fluorophores for enhanced SWIR imaging.

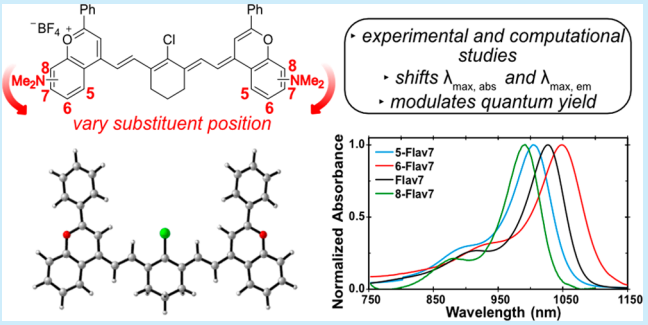

Fluorophores in the shortwave infrared (SWIR, 1000−2000 nm) region of the electromagnetic spectrum have recently garnered excitement as tools for biological imaging.[1−3] The SWIR region is advantageous for optical imaging in complex systems because of the increased depth penetration of light through tissue, enhanced image resolution, and low-energy photons as compared with the visible and near-infrared regions.[4,5] Imaging in the SWIR region originally necessitated single-wall carbon nanotubes (SWCNTs),[6−9] rare-earth nanomaterials,[10−12] or quantum dots[13−15] as contrast agents, which have biocompatibility or bioaccumulation concerns.[11,16−19] In contrast with these nanostructures, small-molecule fluorophores have low toxicity and are readily cleared from the body.[20] However, it is challenging to obtain fluorophores with absorption and emission above 1000 nm with fluorescence quantum yields (Φ_F) greater than ∼0.3%.[21−23]

In 2017, we reported a bright flavylium heptamethine SWIR fluorophore, deemed **Flav7** (**1**, Figure 1).[24] **Flav7** contains a dimethylamino substituent at the seven-position, which provided a λ_{max} above 1000 nm. Recently, we have varied the electron-donating substituent at the seven-position and found that the $\lambda_{max,abs}$ can be modulated by ∼80 nm and form a linear free energy relationship with σ *meta* Hammett constants.[25] The identity of the substituent had a minimal effect on the quantum yield of the series analyzed (Φ_F = 0.42−0.62%). Finding that the seven-position represented the *meta*-position prompted our interest in placing the dimethylamino group at other positions on the flavylium heterocycle (Figure 1). Additional π-donation resulting from *para* and *ortho* substitution can lead to more significant electronic contributions from substituents, although the *ortho*-position can be complicated by sterics.[26] Herein we report how dimethylamino substituents at putative *ortho*-, *meta*- and *para*-positions on

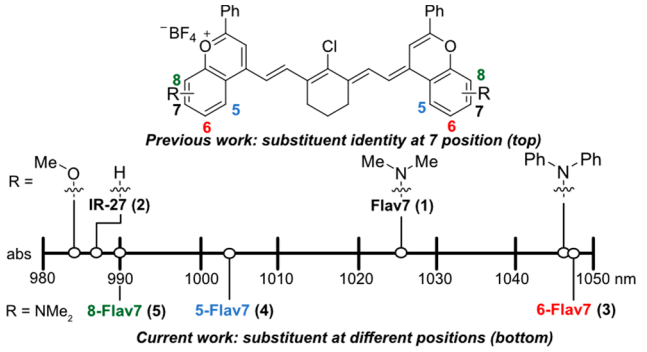

Figure 1. Systematic exploration of structural modifications of Flav7 (**1**). Previous work on derivatives at the seven-position, including methoxy and diphenylamino groups with a shift in λ_{max}.[25] Current work on exploring dimethylamino substitutions at different positions (five-, six-, and eight-) on the heterocycle (**3**−**5**).

flavylium heptamethine fluorophores affect photophysical properties employing experimental and quantum-mechanical analyses.

The dimethylamino flavylium heptamethine dyes were synthesized by leveraging chemistry developed to access **Flav7** derivatives.[25] The dimethylamino group was installed through a Buchwald−Hartwig amination from either triflated

Received: July 3, 2020
Published: July 29, 2020

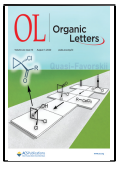

https://dx.doi.org/10.1021/acs.orglett.0c02213
Org. Lett. 2020, 22, 6150−6154

Scheme 1. Synthetic Scheme for Dimethylamino Flavylium Heptamethines 3−5 with Substituents at the Five-, Six-, and Eight-Positions[a]

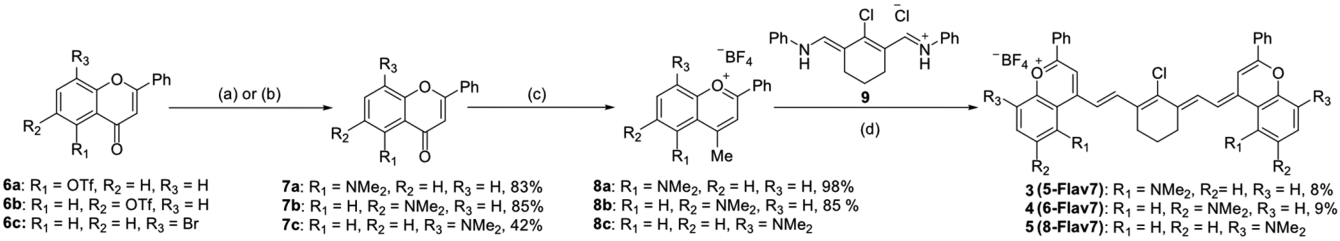

[a](a) RuPhos Pd G3 (0.10 equiv), RuPhos (0.10 equiv), Cs_2CO_3, $HNMe_2$, toluene, 110 °C, 24 h for **6a** and **6b**. (b) SPhos Pd G3 (0.10 equiv), SPhos (0.10 equiv) Cs_2CO_3, $HNMe_2$, toluene, 110 °C, 24 h for **6c**. (c) MeMgBr (1.4 M), THF, r.t. overnight. (d) 2,6-di-*tert*-butyl-4-methylpyridine, *n*-butanol/toluene or acetic anhydride, 100 °C, 10−15 min. Refer to the SI for further experimental details.

or brominated flavones (**6a−c**) to provide dimethylamino substituents at the five-, six-, or eight-position (**7a−c**), respectively (Scheme 1). The addition of methyl-Grignard followed by quenching with tetrafluoroboric acid yielded flavylium heterocycles (**8a−c**), which could then be treated with linker **9** and 2,4-di-*tert*-butyl-4-methylpyridine to provide **5-**, **6-**, and **8-Flav7** (**3−5**, respectively). These dyes are named with the first number representing the position of the dimethylamino substituent on the flavylium heterocycle, and Flav7 references the flavylium heptamethine.

We isolated pure **5-Flav7** (**3**) and **6-Flav7** (**4**). However, the eight-substituted flavylium (**8c**) readily reacted with oxygen to form a monomethine dye, characterized by an absorption peak at 722 nm (Figure S1).[24] To minimize this, crude **8c** was immediately taken to the next reaction. The resulting **8-Flav7** (**5**) proved difficult to purify due to its instability.[27] Thus we gained as much photophysical information as possible from the crude sample. The absorption coefficient (ε) was not determined due to insufficient purity.

We evaluated the photophysical properties of the newly synthesized dyes in comparison with **Flav7** (**1**, Figure 2). The

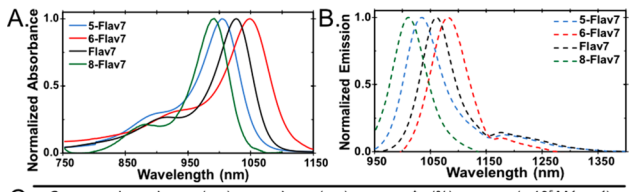

C.

Compound	$\lambda_{max,abs}$ (nm)	$\lambda_{max,em}$ (nm)	Φ_F (%)	ε (x 10^5 M^{-1} cm^{-1})
IR-27 (2)[a]	987	1011	0.35 ± 0.01	2.31 ± 0.06
5-Flav7 (3)	1004	1036	0.14 ± 0.01	0.79 ± 0.09
6-Flav7 (4)	1048	1080	0.12 ± 0.01	1.6 ± 0.3
Flav7 (1)[a]	1027	1053	0.61 ± 0.02	2.41 ± 0.01
8-Flav7 (5)[b]	990	1015	0.16 ± 0.01	N/A

Figure 2. Normalized (A) absorbance and (B) emission of the flavylium polymethine dyes discussed. (C) Photophysical data of unsubstituted (**IR-27**, **2**) and dimethylamino-substituted heptamethine dyes (**1**, **3−5**). All samples were taken in dichloromethane. [a]Data previously reported.[25] [b]Photophysical data were taken with crude sample.

absorbance and emission spectra clearly show that the position of the dimethylamino affects the $\lambda_{max,abs}$ and $\lambda_{max,em}$. Previously, we correlated the seven-position with the *meta*-position through Hammett analysis.[25] We expected that the six-position would correspond to the *para*-position and that substituents at this position would show pronounced effects due to enhanced π-donation. Indeed, we observed this result, as **6-Flav7** (**4**, Figure 2, red) is 20 nm bathochromically shifted from **Flav7** (**1**, Figure 2, black).

We then reasoned that the five-position could serve as the other *meta*-position and the eight-position would be the *ortho*-position. We expected that the absorption and emission of **5-Flav7** (**3**) would be similar to those of **Flav7** (**1**), and the same comparison could be drawn for **8-Flav7** (**5**) and **6-Flav7** (**4**). However, we observed that both **3** and **5** were hypsochromically shifted in comparison with **Flav7** (**1**). **5-Flav7** (**3**, Figure 2, blue) has a $\lambda_{max,abs}$ of 1004 nm, a blue shift of 23 nm from **Flav7** (**1**). **8-Flav7** (**5**, Figure 2, green) has a $\lambda_{max,abs}$ at 990 nm, nearly identical to parent dye **IR-27** (**2**). These results were counterintuitive to the predicted $\lambda_{max,abs}$ based on Hammett parameters and prompted a quantum-mechanical study.

We performed a conformational search of 10 000 structures enforcing the all-*trans* configuration along the polymethine chain while searching the conformational flexibility of the phenyl groups. (Refer to the SI.) We optimized the ten lowest conformers of each molecule with the M06-2X[28] density functional and the 6-31+G(d,p) basis set. We used the integral equation formalism polarizable continuum model (IEFPCM)[29] for all calculations in the presence of dichloromethane. The computed range of free energies between the ten lowest energy conformers is 0.0 to 0.7 kcal mol^{-1} (Figure S2).

To evaluate the photophysical properties, we used the global minima for **Flav7** dyes (**1**, **3−5**) as well as unmodified **IR-27** (**2**). The conjugated C−C bonds in the polymethine chains ranged from 1.39 to 1.41 Å. However, the substituents altered the planarity of the π-system along the polymethine chain and the flavylium heterocycle. We deconvoluted these effects with two angular parameters, α and β (Figure 3A,B). We define α as the angle between the plane of the polymethine and the plane of the flavylium, whereas β is the angle between the plane of the flavylium and the substituent. Analysis of the α angles shows little distortion between the polymethine plane and the flavylium heterocycles when the dimethylamino group is at the six-, seven-, or eight-position (α = 5−7°, Figure 3B). At the five-position, the NMe_2 C−H bonds clash with the vinyl C−H bond of the polymethine chain, which results in a larger angle of 18°.

The NMe_2 substituents also alter the geometries near the vicinity of the flavylium heterocycle. The torsion angle β in **Flav7** (**1**) and **6-Flav7** (**4**) are nearly planar (5° and 1°, respectively). **5-Flav7** (**3**) and **8-Flav7** (**5**) have β angles of 46° and 44°, respectively, which indicate significant out-of-plane distortions. The NMe_2 groups rotate to minimize closed-shell repulsion to the vinyl C−H bond in **5-Flav7** (**3**, Figure

https://dx.doi.org/10.1021/acs.orglett.0c02213
Org. Lett. 2020, 22, 6150−6154

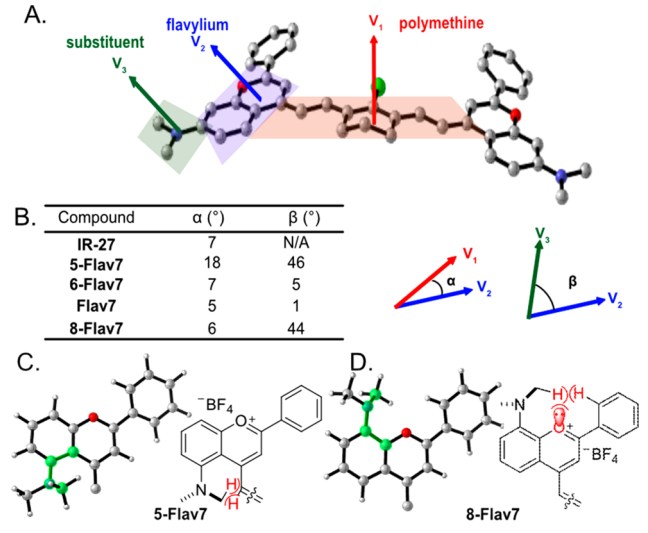

Figure 3. (A) Represented by **Flav7**; torsion angles are defined by α (V_1 to V_2, red to blue) and β (V_3 to V_2, green to blue) using the normal of the plane of the polymethine (V_1), flavylium (V_2), and substituent (V_3). (B) Table of α and β angles for **Flav7** dyes. (C,D) Heterocycle structures of (C) **5-Flav7** and (D) **8-Flav7** at the S_0 state, optimized with M06-2X/6-31+G(d,p). The polymethine chain is omitted for clarity. The dihedral angles at the substituted positions of the flavylium heterocycles are highlighted in green to show the rotation of the NMe_2 group in **5-Flav7** and **8-Flav7**.

3C) and to the oxygen lone pair and adjacent C−H bond of the phenyl group in **8-Flav7** (**5**, Figure 3D).

We computed the frontier molecular orbitals (FMOs) to illustrate the differences in the electronic structures of these fluorophores. Displayed in Figure 4A and Figure S3 are the highest occupied molecular orbitals and lowest unoccupied

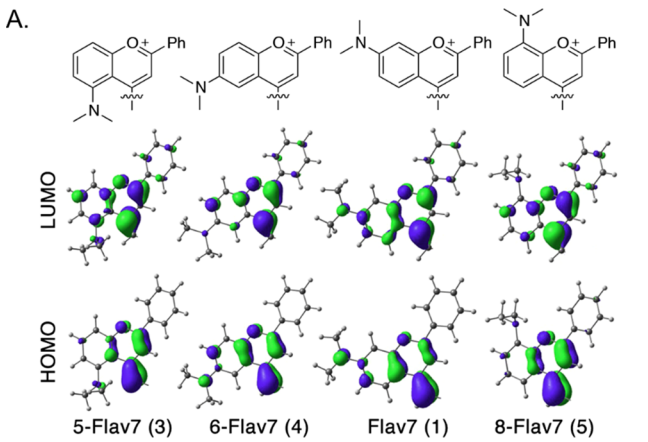

B.

Compound	Δ (nm)	HOMO-LUMO gap (eV)	$\lambda_{max,\ calc.\ abs}$ (nm)
IR-27 (2)	165	3.03	822
5-Flav7 (3)	169	2.99	835
6-Flav7 (4)	190	2.94	858
Flav7 (1)	163	2.98	864
8-Flav7 (5)	159	3.03	831

Figure 4. (A) HOMOs and LUMOs of **Flav7** (**1**) and (**5**, **6**, and **8**)-**Flav7** (**3**−**5**) at the M06-2X/6-31+G(d,p) level of theory. Polymethine chains were omitted for clarity. Explicit frontier molecular orbital information can be found in the SI. (B) Table of calculated $\lambda_{max,calc,abs}$ (nm) determined by the theoretical HOMO−LUMO gap (eV). Δ is the difference between experimental and calculated $\lambda_{max,abs}$.

molecular orbitals (HOMOs and LUMOs). The FMOs show that the extent of π-conjugation in the flavylium heterocycles varies with respect to the substituent site. **Flav7** (**1**) and **6-Flav7** (**4**) have dimethylamino substituents that are nearly coplanar with flavylium heterocycles, allowing for the NMe_2 to maximally extend the orbital overlap in the HOMOs and LUMOs. This results in reduced HOMO−LUMO gaps and longer $\lambda_{max,abs}$. The 46° out-of-plane torsion in **5-Flav7** (**3**) results in decreased π-conjugation of the nitrogen lone pair to the chromophore. The substantial out-of-plane distortion of **8-Flav7** (**5**) nearly eliminates the π-conjugation of the nitrogen lone pair, which leads to unperturbed $\lambda_{max,abs}$ relative to the parent dye, **IR-27** (**2**).

The predicted $\lambda_{max,abs}$ values of dyes were calculated using the configuration interactions of singles with corrections to doubles method (CIS(D))[30,31] and the cc-pVDZ basis sets. The computed HOMO−LUMO gaps match the experimentally observed trend (Figure 4B). **6-Flav7** (**4**) has the smallest gap (2.94 eV), which correlates with the longest $\lambda_{max,abs}$, whereas **8-Flav7** (**5**) has the largest gap (3.03 eV) and the shortest experimentally determined $\lambda_{max,abs}$. The predicted $\lambda_{max,abs}$ is systematically blue-shifted 159−190 nm relative to experimental results, likely due to contributions from double excitation that are unaccounted for with single-reference quantum-mechanical methods.[32,33]

Our analysis of the λ_{max} shows that the position of substituents on the flavylium ring can affect λ_{max}, comparable to the magnitude observed by varying the electronics at the seven-position. However, the major limitation of small-molecule fluorophores in the SWIR is their low Φ_F.[21] At 0.61%, **Flav7** (**1**) has a respectable Φ_F for polymethine SWIR fluorophores. It is of interest to gain an understanding of how structural modifications impact Φ_F to develop brighter probes. Previously, we found that functional groups at the seven-position showed little change in the quantum yield of fluorescence.[25] However, here we see that the substituent placement can greatly alter the Φ_F (Figure 2).

We measured Φ_F values for **5-Flav7**, **6-Flav7**, and **8-Flav7** (**3**−**5**). All three were significantly less fluorescent than **Flav7** (**1**), with Φ_F ranging from 0.12 to 0.16%. We were particularly interested in the large difference between **Flav7** (**1**) and **6-Flav7** (**4**), which are conformationally similar. Flavylium heterocycles are structurally similar to coumarin heterocycles, and large differences in Φ_F between six- and seven-position-substituted coumarin fluorophores have previously been observed.[27] The low Φ_F in 6-aminocoumarins (**10**) compared with 7-aminocoumarins (**11**) was attributed to a more significant contribution of a twisted intermolecular charge-transfer (TICT) state in which the amine donor twists out of plane by ~90° upon photoexcitation, forming a nonemissive species.[34,35] We hypothesized that a similar phenomenon could contribute to the loss of fluorescence in **6-Flav7** (**4**), as compared with the parent **Flav7** (**1**).

To gain insight into whether TICT was contributing to observed differences in fluorescence in **1** and **4**, we synthesized a flavylium heptamethine that contained an azetidine at the six-position. Azetidines have been been shown to minimize TICT states by preventing the substituent from twisting out of plane.[36] **Azet-6-Flav7** (**12**, Figure 5A) was synthesized following a similar procedure to 6-Flav7 (Scheme S1). We found the Φ_F to be 0.21%, 1.75 times higher than the dimethylamino derivative. In contrast, azetidine at the seven-position (**13**) resulted in a slight decrease in Φ_F compared with

https://dx.doi.org/10.1021/acs.orglett.0c02213
Org. Lett. 2020, 22, 6150−6154

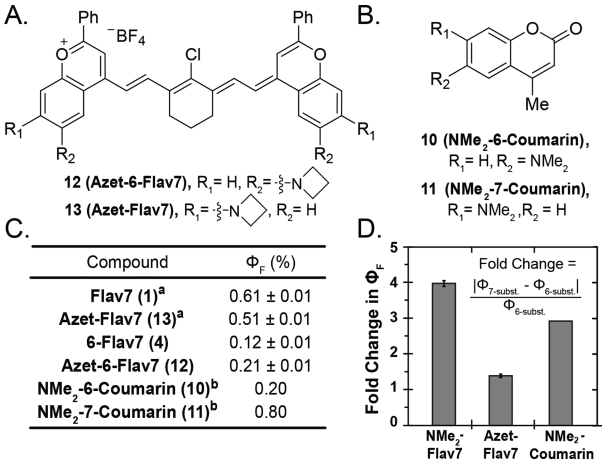

Compound	Φ_F (%)
Flav7 (1)[a]	0.61 ± 0.01
Azet-Flav7 (13)[a]	0.51 ± 0.01
6-Flav7 (4)	0.12 ± 0.01
Azet-6-Flav7 (12)	0.21 ± 0.01
NMe_2-6-Coumarin (10)[b]	0.20
NMe_2-7-Coumarin (11)[b]	0.80

Figure 5. (A) Structures of azetidine-substituted flavylium heptamethine dyes (**12**, **13**). (B) Structures of 6- and 7-aminocoumarin fluorophores (**10**, **11**). (C) Φ_F of flavylium heptamethine and coumarin dyes in dichloromethane and decanol, respectively. [a]Previously reported.[25] [b]Previously reported.[34] (D) Fold change of Φ_F between six- and seven-substituted flavylium heptamethine or coumarin fluorophores.

Flav7 (**1**) (0.51 vs 0.61%, Figure 5C).[25] We calculated the fold change in Φ_F for each of the pairs of six- and seven-substituted fluorophores (**4** vs **1**, **12** vs **13**, **10** vs **11**; Figure 5D) and found that the NMe_2 variants of both flavylium heptamethine and coumarin dyes had similar changes, whereas the azetidine-functionalized Flav7 dyes displayed a reduced change. These data support the notion that TICT could be playing a larger role at the six-position, contributing to the observed difference in Φ_F between **Flav7** (**1**) and **6-Flav7** (**4**).

In conclusion, we have demonstrated that dimethylamino substituent placement significantly influences the photophysical properties of flavylium heptamethine dyes. Substituent steric effects impact the degree of conjugation and alter the $\lambda_{max,abs}$. We have used density functional theory calculations to understand the origin of these unique photophysical properties. The seven-position appears to be advantageous for obtaining a high quantum yield and maintaining SWIR absorption maxima; however, further red-shifted dyes can be obtained by substituting the six-position. The insights garnered herein can contribute to the design of novel fluorophores to be utilized for high-resolution SWIR *in vivo* imaging.

■ ASSOCIATED CONTENT

Supporting Information

The Supporting Information is available free of charge at https://pubs.acs.org/doi/10.1021/acs.orglett.0c02213.

Experimental procedures, Figures S1−S3, Scheme S1, and full spectroscopic data and computational analysis for compounds (PDF)

■ AUTHOR INFORMATION

Corresponding Authors

Steven A. Lopez − *Department of Chemistry and Chemical Biology, Northeastern University, Boston, Massachusetts 02115, United States;* orcid.org/0000-0002-8418-3638; Email: s.lopez@northeastern.edu

Ellen M. Sletten − *Department of Chemistry and Biochemistry, University of California, Los Angeles, Los Angeles, California 90095, United States;* orcid.org/0000-0002-0049-7278; Email: sletten@chem.ucla.edu

Authors

Monica Pengshung − *Department of Chemistry and Biochemistry, University of California, Los Angeles, Los Angeles, California 90095, United States*

Jingbai Li − *Department of Chemistry and Chemical Biology, Northeastern University, Boston, Massachusetts 02115, United States*

Fatemah Mukadum − *Department of Chemistry and Chemical Biology, Northeastern University, Boston, Massachusetts 02115, United States*

Complete contact information is available at: https://pubs.acs.org/10.1021/acs.orglett.0c02213

Author Contributions

M.P. and E.M.S. designed the study. M.P. performed the synthesis and measured the photophysical properties. J.L. and F.M. performed the quantum mechanical calculations, and J.L. completed the analysis of the substituent effects on the photophysical properties. M.P., J.L., S.A.L., and E.M.S, wrote and edited the paper. All authors have given approval to the final version of the manuscript.

Notes

The authors declare no competing financial interest.

■ ACKNOWLEDGMENTS

This work was supported by grants from the Sloan Foundation (FG-2018-10855 to E.M.S.), NIH (1R01EB027172-01 to E.M.S.), and NSF (NSF-1940307 to S.A.L.; CHE-1905242 to E.M.S.). Instrumentation was funded through the NSF MRI (CHE-1048804) and NIH (1S10OD016387-01). S.A.L, and J.L. acknowledge the Massachusetts Green High-Performance Computing Center (MGHPCC) for computing resources and the staff of Research Computing for support. We thank Dr. J. Cox (Northeastern), P. Neal (Northeastern), I. Lim (UCLA), and E. Cosco (UCLA) for helpful discussions.

■ REFERENCES

(1) Schnermann, M. J. Organic Dyes for Deep Bioimaging. *Nature* **2017**, *551*, 176−177.

(2) Thimsen, E.; Sadtler, B.; Berezin, M. Y. Shortwave-Infrared (SWIR) Emitters for Biological Imaging: A Review of Challenges and Opportunities. *Nanophotonics* **2017**, *6* (5), 1043−1054.

(3) Weissleder, R. A Clearer Vision for in Vivo Imaging. *Nat. Biotechnol.* **2001**, *19* (4), 316−317.

(4) Smith, A. M.; Mancini, M. C.; Nie, S. Bioimaging: Second Window for in Vivo Imaging. *Nat. Nanotechnol.* **2009**, *4*, 710−711.

(5) Carr, J. A.; Franke, D.; Caram, J. R.; Perkinson, C. F.; Saif, M.; Askoxylakis, V.; Datta, M.; Fukumura, D.; Jain, R. K.; Bawendi, M. G.; Bruns, O. T. Shortwave Infrared Fluorescence Imaging with the Clinically Approved Near-Infrared Dye Indocyanine Green. *Proc. Natl. Acad. Sci. U. S. A.* **2018**, *115* (17), 4465−4470.

(6) Hong, G.; Lee, J. C.; Robinson, J. T.; Raaz, U.; Xie, L.; Huang, N. F.; Cooke, J. P.; Dai, H. Multifunctional in Vivo Vascular Imaging Using Near-Infrared II Fluorescence. *Nat. Med.* **2012**, *18* (12), 1841−1846.

(7) Welsher, K.; Liu, Z.; Sherlock, S. P.; Robinson, J. T.; Chen, Z.; Daranciang, D.; Dai, H. A Route to Brightly Fluorescent Carbon Nanotubes for Near-Infrared Imaging in Mice. *Nat. Nanotechnol.* **2009**, *4* (11), 773−780.

(8) Diao, S.; Blackburn, J. L.; Hong, G.; Antaris, A. L.; Chang, J.; Wu, J. Z.; Zhang, B.; Cheng, K.; Kuo, C. J.; Dai, H. Fluorescence

Imaging In Vivo at Wavelengths beyond 1500 nm. *Angew. Chem., Int. Ed.* **2015**, *54* (49), 14758−14762.
(9) Robinson, J. T.; Hong, G.; Liang, Y.; Zhang, B.; Yaghi, O. K.; Dai, H. In Vivo Fluorescence Imaging in the Second Near-Infrared Window with Long Circulating Carbon Nanotubes Capable of Ultrahigh Tumor Uptake. *J. Am. Chem. Soc.* **2012**, *134* (25), 10664−10669.
(10) Naczynski, D. J.; Tan, M. C.; Zevon, M.; Wall, B.; Kohl, J.; Kulesa, A.; Chen, S.; Roth, C. M.; Riman, R. E.; Moghe, P. V. Rare-Earth- Doped Biological Composites as in Vivo Shortwave Infrared Reporters. *Nat. Commun.* **2013**, *4*, 2199.
(11) Naczynski, D. J.; Tan, M. C.; Riman, R. E.; Moghe, P. V. Rare Earth Nanoprobes for Functional Biomolecular Imaging and Theranostics. *J. Mater. Chem. B* **2014**, *2*, 2958−2973.
(12) Naczynski, D. J.; Sun, C.; Türkcan, S.; Jenkins, C.; Koh, A. L.; Ikeda, D.; Pratx, G.; Xing, L. X-Ray-Induced Shortwave Infrared Biomedical Imaging Using Rare-Earth Nanoprobes. *Nano Lett.* **2015**, *15* (1), 96−102.
(13) Bruns, O. T.; Bischof, T. S.; Harris, D. K.; Franke, D.; Shi, Y.; Riedemann, L.; Bartelt, A.; Jaworski, F. B.; Carr, J. A.; Rowlands, C. J.; et al. Next-Generation in Vivo Optical Imaging with Short-Wave Infrared Quantum Dots. *Nat. Biomed. Eng.* **2017**, *1* (4), 0056.
(14) Dong, B.; Li, C.; Chen, G.; Zhang, Y.; Zhang, Y.; Deng, M.; Wang, Q. Facile Synthesis of Highly Photoluminescent Ag_2Se Quantum Dots as a New Fluorescent Probe in the Second Near-Infrared Window for in Vivo Imaging. *Chem. Mater.* **2013**, *25* (12), 2503−2509.
(15) Hong, G.; Robinson, J. T.; Zhang, Y.; Diao, S.; Antaris, A. L.; Wang, Q.; Dai, H. In Vivo Fluorescence Imaging with Ag_2S Quantum Dots in the Second Near-Infrared Region. *Angew. Chem., Int. Ed.* **2012**, *51* (39), 9818−9821.
(16) Yang, S. T.; Wang, X.; Jia, G.; Gu, Y.; Wang, T.; Nie, H.; Ge, C.; Wang, H.; Liu, Y. Long-Term Accumulation and Low Toxicity of Single-Walled Carbon Nanotubes in Intravenously Exposed Mice. *Toxicol. Lett.* **2008**, *181* (3), 182−189.
(17) Liu, Z.; Davis, C.; Cai, W.; He, L.; Chen, X.; Dai, H. Circulation and Long-Term Fate of Functionalized, Biocompatible Single-Walled Carbon Nanotubes in Mice Probed by Raman Spectroscopy. *Proc. Natl. Acad. Sci. U. S. A.* **2008**, *105* (5), 1410−1415.
(18) Soo Choi, H.; Liu, W.; Misra, P.; Tanaka, E.; Zimmer, J. P; Itty Ipe, B.; Bawendi, M. G; Frangioni, J. V Renal Clearance of Quantum Dots. *Nat. Biotechnol.* **2007**, *25* (10), 1165−1170.
(19) Fitzpatrick, J. A. J.; Andreko, S. K.; Ernst, L. A.; Waggoner, A. S.; Ballou, B.; Bruchez, M. P. Long-Term Persistence and Spectral Blue Shifting of Quantum Dots in Vivo. *Nano Lett.* **2009**, *9* (7), 2736−2741.
(20) Lavis, L. D.; Raines, R. T. Bright Ideas for Chemical Biology. *ACS Chem. Biol.* **2008**, *3* (3), 142−155.
(21) Casalboni, M.; De Matteis, F.; Prosposito, P.; Quatela, A.; Sarcinelli, F. Fluorescence Efficiency of Four Infrared Polymethine Dyes. *Chem. Phys. Lett.* **2003**, *373* (3−4), 372−378.
(22) Wang, S.; Fan, Y.; Li, D.; Sun, C.; Lei, Z.; Lu, L.; Wang, T.; Zhang, F. Anti-Quenching NIR-II Molecular Fluorophores for in Vivo High-Contrast Imaging and PH Sensing. *Nat. Commun.* **2019**, *10* (1), 1058.
(23) Hong, G.; Zou, Y.; Antaris, A. L.; Diao, S.; Wu, D.; Cheng, K.; Zhang, X.; Chen, C.; Liu, B.; He, Y.; et al. Ultrafast Fluorescence Imaging in Vivo with Conjugated Polymer Fluorophores in the Second Near-Infrared Window. *Nat. Commun.* **2014**, *5* (1), 4206−9.
(24) Cosco, E. D.; Caram, J. R.; Bruns, O. T.; Franke, D.; Day, R. A.; Farr, E. P.; Bawendi, M. G.; Sletten, E. M. Flavylium Polymethine Fluorophores for Near- and Shortwave Infrared Imaging. *Angew. Chem., Int. Ed.* **2017**, *56* (42), 13126−13129.
(25) Cosco, E. D.; Spearman, A. L.; Ramakrishnan, S.; Lingg, J. G. P.; Saccomano, M.; Pengshung, M.; Arus, B. A.; Wong, K. C. Y.; Glasl, S.; Ntziachristos, V.; Warmer, M.; McLaughlin, R. R.; Bruns, O. T.; Sletten, E. M. Shortwave infrared polymethine fluorophores matched to excitation lasers enable noninvasive, multicolor *in vivo* imaging in real time. *Nat. Chem.* **2020**, in revision.
(26) Hansch, C.; Leo, A.; Taft, R. W. A Survey of Hammett Substituent Constants and Resonance and Field Parameters. *Chem. Rev.* **1991**, *91*, 165−195.
(27) Purification of 8-Flav7 was attempted via silica column chromatography, HPLC, recrystallization, and washing with solvents (toluene, tetrahydrofuran, diethyl ether, and ethyl acetate).
(28) Zhao, Y.; Truhlar, D. G. The M06 Suite of Density Functionals for Main Group Thermochemistry, Thermochemical Kinetics, Noncovalent Interactions, Excited States, and Transition Elements: Two New Functionals and Systematic Testing of Four M06-Class Functionals and 12 Other Functionals. *Theor. Chem. Acc.* **2008**, *120* (1−3), 215−241.
(29) Scalmani, G.; Frisch, M. J. Continuous Surface Charge Polarizable Continuum Models of Solvation. I. General Formalism. *J. Chem. Phys.* **2010**, *132* (11), 114110.
(30) Head-Gordon, M.; Rico, R. J.; Oumi, M.; Lee, T. J. A Doubles Correction to Electronic Excited States from Configuration Interaction in the Space of Single Substitutions. *Chem. Phys. Lett.* **1994**, *219* (1−2), 21−29.
(31) Head-Gordon, M.; Maurice, D.; Oumi, M. A Perturbative Correction to Restricted Open Shell Configuration Interaction with Single Substitutions for Excited States of Radicals. *Chem. Phys. Lett.* **1995**, *246* (1−2), 114−121.
(32) Zhou, P. Why the Lowest Electronic Excitations of Rhodamines Are Overestimated by Time-Dependent Density Functional Theory. *Int. J. Quantum Chem.* **2018**, *118* (23), No. e25780.
(33) CIS(D) leads to smaller deviations relative to TD-DFT methods because of the built-in corrections to the doubly excited state.
(34) Rettig, W.; Klock, A. Intramolecular Fluorescence Quenching in Aminocoumarines. Identification of an Excited State with Full Charge Separation. *Can. J. Chem.* **1985**, *63*, 1649−1653.
(35) An azetidine substituted at the seven-position of coumarin has been previously synthesized and has shown some TICT character in water. Grimm, J. B.; English, B. P.; Chen, J.; Slaughter, J. P.; Zhang, Z.; Revyakin, A.; Patel, R.; Macklin, J. J.; Normanno, D.; Singer, R. H.; et al. A General Method to Improve Fluorophores for Live-Cell and Single-Molecule Microscopy. *Nat. Methods* **2015**, *12* (3), 244−250.
(36) Liu, X.; Qiao, Q.; Tian, W.; Liu, W.; Chen, J.; Lang, M. J.; Xu, Z. Aziridinyl Fluorophores Demonstrate Bright Fluorescence and Superior Photostability by Effectively Inhibiting Twisted Intramolecular Charge Transfer. *J. Am. Chem. Soc.* **2016**, *138*, 6960−6963.

NOTE ADDED AFTER ASAP PUBLICATION

Figure 5 was corrected on July 30, 2020.

https://dx.doi.org/10.1021/acs.orglett.0c02213
Org. Lett. 2020, 22, 6150−6154